



ISSN: 0976-3031

Available Online at <http://www.recentscientific.com>

CODEN: IJRSFP (USA)

International Journal of Recent Scientific Research  
Vol. 10, Issue, 01(A), pp. 30242-30247, January, 2019

**International Journal of  
Recent Scientific  
Research**

DOI: 10.24327/IJRSR

## Research Article

# THERMAL, PHYSICAL AND STRUCTURAL PROPERTIES OF MIXED ALKALI AND TRANSITION METAL IONS IN SODIUM BORATE GLASS

Rajesh S<sup>1\*</sup> and Palani R<sup>2</sup>

<sup>1</sup>Department of Physics, Indian Arts and Science College, Tiruvannamalai - 606 802

<sup>2</sup>Department of Physics, Annamalai University, Chidambaram - 608002

DOI: <http://dx.doi.org/10.24327/ijrsr.2019.1001.3015>

### ARTICLE INFO

#### Article History:

Received 15<sup>th</sup> October, 2018

Received in revised form 7<sup>th</sup>

October, 2018

Accepted 13<sup>th</sup> December, 2018

Published online 28<sup>th</sup> January, 2019

#### Key Words:

Sodium borate glasses, X-ray diffractometry, Thermo gravimetric analysis, Differential thermal analysis, Microhardness and Fourier transform infrared spectroscopy.

### ABSTRACT

Glasses with composition  $20\text{Na}_2\text{O}-(80-x)\text{B}_2\text{O}_3-x\text{Li}_2\text{O}$  and  $20\text{Na}_2\text{O}-(80-x)\text{B}_2\text{O}_3-x\text{WO}_3$  (where  $x = 0$  to 10 in steps 2 mol%) were characterized by the amorphous nature of the samples were ascertained using X-ray diffractometry (XRD), thermo gravimetric analysis (TGA), differential thermal analysis (DTA), microhardness and Fourier transform infrared spectroscopy (FTIR). The amorphous phase of the prepared glass samples was confirmed from their TGA, and DTA profiles. DTA profile yielded data of transition temperature ( $T_g$ ), crystallization temperature ( $T_p$ ) and the thermal stability ( $\Delta T$ ) range of glasses. Microhardness studies exposed that the hardness of the sodium borate glass increases with an increase in applied load as well as with the doping of alkali and transition metal ions. Meyer's index number/work hardening exponent 'n' was calculated and it was found that the material belongs to hard material category. FTIR spectra of the glasses were interpreted in terms of the structural transformations on the glass network by the changing composition. FTIR spectral study reveals the existence of  $\text{BO}_3$  and  $\text{BO}_4$  groups with Li-O-Li and W-O-W vibrations in the present glasses. The presence of varied types like di, tetra, penta, and ortho borate groups are confirmed in the glass matrix.

Copyright © Rajesh S and Palani R, 2019, this is an open-access article distributed under the terms of the Creative Commons Attribution License, which permits unrestricted use, distribution and reproduction in any medium, provided the original work is properly cited.

## INTRODUCTION

The alkali-borate glasses are commonly used materials in the field of opto-acoustical electronics, in nonlinear devices for frequency conversion in the ultraviolet region and piezoelectric actuator. Meanwhile, these glasses and their crystalline counterparts are considered to be good candidates for the optically induced elasto-opticity (Saddeek *et al*, 2007). Alkali borate glasses have been studied for various technical and industrial applications. The insulating property of borate glasses turns into a semiconducting or electronic or ion conducting nature when metal oxides such as alkali and alkaline earth oxides are added to them. Alkali borate glass systems are good candidates for ion conduction and suitable for the fabrication of solid state batteries (Balachandar *et al*, 2013). Borate glasses, based on  $\text{B}_2\text{O}_3$  network may provide an alternative bioactive glass for biomedical applications. The structure of borate glass not only depends on the glass forming oxides, but also on the glass modifier oxides and doping salts present in the glass composition. Among them, tungsten oxide is of intense interest and has been investigated extensively for its distinctive properties. With outstanding electrochromic,

photo-chromic, gas chromic, gas sensor, photo-catalyst and photoluminescence properties, tungsten oxide has been used to construct 'smart window', anti-glare rear view mirrors for automobiles, non-emissive displays, optical recording devices, solid state gas sensors, humidity and temperature sensors, biosensors, photonic crystals and so forth. The tungsten ion exists in different valence states  $\text{W}^{6+}$ ,  $\text{W}^{5+}$ ,  $\text{W}^{4+}$ , etc. Hence its doping can affect the structure and optical properties of host glasses (Saravenan *et al*, 2015). Doping of materials with lithium ion is technologically very significant. It is important in preparation of optical waveguides and other optoelectronic elements (Lawrence *et al*, 2005). Borate glasses containing  $\text{Li}^+$  have been extensively studied due to their technological applications as solid electrolyte in electrochemical devices such as batteries (Abdel *et al*, 2008).

Thermal analytical methods monitor the changes in some physical property such as weight, enthalpy or dimensions or mechanical, electrical, acoustic or properties of the sample as it is subjected to a programmed heating from an initial lower temperature to a final higher temperature at a specified heating rate. The most commonly used techniques include

\*Corresponding author: Rajesh S

Department of Physics, Indian Arts and Science College, Tiruvannamalai - 606 802

thermogravimetry analysis (TGA), differential thermal analysis (DTA) and differential scanning calorimeter (DSC). Thermal events that may occur in the sample as it is undergoing a change in temperature include (i) phase transitions (ii) melting (iii) sublimation (iv) decomposition (v) glass transition in polymers (vi) oxidation/reduction (vii) combustion (viii) heterogeneous catalysis and (xi) addition/combination. These thermal events may be studied by the use of appropriate thermal analytical techniques. Application of TGA and DTA include qualitative analysis and quantitative analysis as well as study of the thermal stability of glass substances.

Hardness is a measure of the resistance of a material to be penetrated and eroded by sharp projections of other materials (Varshneya *et al*, 1994). Hardness of any material is the result of a complex process of deformation during indentation, the nature of which is more cryptic in the case of glasses because of the limited knowledge of the glass structure (Burkhard *et al*, 2004). During the process of indentation the material undergoes both compression and shear resulting in the observed deformation. Which comprises elastic deformation, flow and densification (Yamane *et al*, 1974). Microhardness is the resistance of network against elastic and plastic deformation as well as against compression. Microhardness is an important parameter often used to define the mechanical properties of a material on a microscopic scale. Measurement of hardness using a diamond pyramid has long been a practical quality control tool for industry (Mander *et al*, 1991).

Fourier transform infrared (FTIR) technique is one of the most sought spectroscopic investigations to probe the structural units present in the glass matrix. To the best of our knowledge, there are no detailed reports on thermal and structural studies on mixed alkali and transition metal ion sodium borate glasses. In the present paper  $20\text{Na}_2\text{O}-(80-x)\text{B}_2\text{O}_3-x\text{Li}_2\text{O}$  and  $20\text{Na}_2\text{O}-(80-x)\text{B}_2\text{O}_3-x\text{WO}_3$  (where  $x = 0$  to  $10$  in steps of  $2$  mol%), glasses are undertaken by using various thermal and spectroscopic techniques to get comprehensive view.

## Experimental

### X-ray diffraction

The amorphous nature of glass samples was confirmed by X-ray diffraction technique using an x-ray diffractometer (MODE: PW3040/60 X'PERT PRO).

### TGA and DTA Measurements

In thermal study, instrument NETZSCH STA 449F3 jupiter analyzer with heating rate of  $20\text{ K min}^{-1}$  in the temperature range of  $20-1000\text{ }^\circ\text{C}$ , under  $\text{N}_2$  gas ambient was used. The glass transition temperatures ( $T_g$ ) were taken as the inflection point of the endothermic change of the calorimetric signal. Crystallization onset temperatures ( $T_p$ ) were specified as the beginning of the reaction where the crystallization first starts and peak temperatures represent the maximum value of the exothermic. Samples amounts of  $32-38\text{ mg}$  were used during DTA measurements. The same instrument has been used for TGA measurement.

The thermal stability of glasses can be described by  $\Delta T$ , which is defined as

$$\Delta T = T_p - T_g \quad \dots (1)$$

Where  $\Delta T$  gives the information about the devitrification tendency of the glasses. The difference between the glass transition temperature and the first exothermic peak onset crystallization temperature,  $\Delta T$ , has been commonly used as a rough criterion of the glass thermal stability against devitrification.

### Microhardness Measurements

The microhardness of the investigated glass samples was measured by using Vicker's microhardness indenter (SHIMADZU HMV-2 series, Japan). Five indentation readings were made and measured for each glass sample. Testing was made using a load of  $100\text{g}$ ,  $200\text{g}$ ,  $300\text{g}$ ,  $500\text{g}$ ,  $1.0\text{Kg}$ ; loading time was fixed for all glass samples ( $15\text{s}$ ). The vicker's microhardness value was calculated from the following equation:

Vicker's microhardness value ( $H_v$ ) (Chenthamarai *et al*, 2001) has been calculated using

$$H_v = 1.8544 P/d^2 \quad \dots (2)$$

Where,  $P$  is the applied load,  $d$  is the mean diagonal length of the indentation impression and  $1.8544$  is a constant, a geometrical factor/ Vicker's conversion factor for the diamond pyramid.

According to Meyer's law (Bull *et al*, 1989), the relation connecting the applied load is given by

$$P = ad^n \quad \dots (3)$$

Where, 'n' is the Meyer's index number or work hardening exponent and 'a' is a constant for a given material. The value of work hardening exponent ( $n$ ) was estimated from the plot of  $\log P$  versus  $\log d$  by the principle least square. The 'n' value is useful to determine whether the material is hard or soft.

### FTIR Measurement

In order to reveal the structural of the glass network, room temperature Fourier transform infrared measurement has been performed with a Bruker Optik GmbH, TENSOR 27, utilizing Middle-infrared light (MIR) excitation Source within the range of  $400-4000\text{ cm}^{-1}$  using the KBr pellet technique. For each spectrum  $64$  scans were made and the spectral resolution of  $4\text{ cm}^{-1}$ .

## RESULTS AND DISCUSSION

### X-ray Diffraction

The X-ray diffraction patterns (Fig.1) of the studied glass systems reveals the absence of any discrete or continuous sharp crystalline peaks, but show homogenous glassy characters.

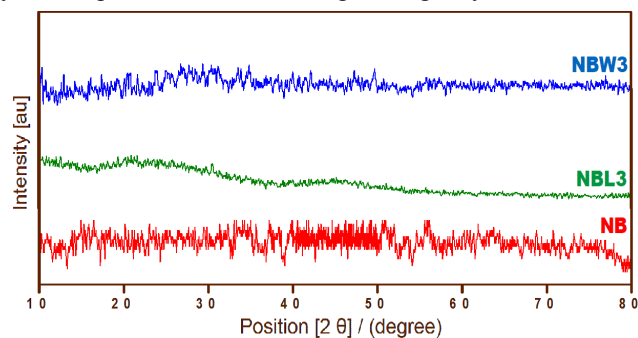


Figure 1 XRD Profile of glass samples of NB, NBL3 and NBW3.

## Thermal Studies

The TGA and DTA profile of the prepared glasses of NB, NBL, and NBW are shown in the Figs.4-6. The TGA profile has shown only considerable weight loss which is less than of 20%. Meanwhile from the DTA, profile of the host glass (Figs.2-4), three important temperatures; glass transition temperature ( $T_g$ ), crystallization temperature ( $T_p$ ) and melting temperature ( $T_m$ ) were identified. The glass transition temperature ( $T_g$ ) is one of the basic characterizing properties of the glass and it confirms the amorphous nature of the glass as XRD (Upender *et al.*, 2011). Table-1 listed out some of the obtained physical quantities value of the host glass.

From the table-1 it is seen that all the value of  $T_g$ ,  $T_p$  and  $T_m$  are increases with the doping of  $Li_2O$  and  $WO_3$  content in sodium borate glass system. From the DTA scans, it is also observed that the lack of sharp endothermic and exothermic peaks evidently specify the formation of homogeneous glass. The change in the glass transition temperature  $T_g$  clearly shows that doping of  $Li_2O$  and  $WO_3$  affects the glass structure. Specifically an increase in  $T_g$  with the addition of  $Li_2O$  and  $WO_3$  contents indicates increase in the rigidity of the glass network (Table-1). The analysis of these results indicates the increase in  $T_g$  with the addition of  $Li_2O$  and  $WO_3$  content might be associated with the augmented cross-link density of various micro-structural groups and closeness of their packing (Sathyanarayana *et al.*, 2013). Further, it has been known from the literature of the glasses that when a higher cross-link density of cation is replaced by a cation of lower cross-link density,  $T_g$  of respective glasses should decrease (Upender *et al.*, 2010, Chowdari *et al.*, 1996). But in the present case this behavior was not observed. This could be due to the difference in cross-link densities of  $Li_2O$  and  $WO_3$ . Therefore, the increase in  $T_g$  may be ascribed to the higher bond strength of B-O ( $\approx 808.8$  KJ mol<sup>-1</sup>) and W-O ( $\approx 672$  KJ mol<sup>-1</sup>) in comparison with the bond strengths of Na-O ( $\approx 270$  KJ mol<sup>-1</sup>) and Li-O ( $\approx 322$  KJ mol<sup>-1</sup>) (Gaafar *et al.*, 2009, Lide *et al.*, 2001). The  $T_g$  is also a measure of strength of the glasses (Upender *et al.*, 2012). The thermally stable glasses will have closed packed structure, whereas thermally unstable glasses will have packed structure (Hirashima *et al.*, 1988).

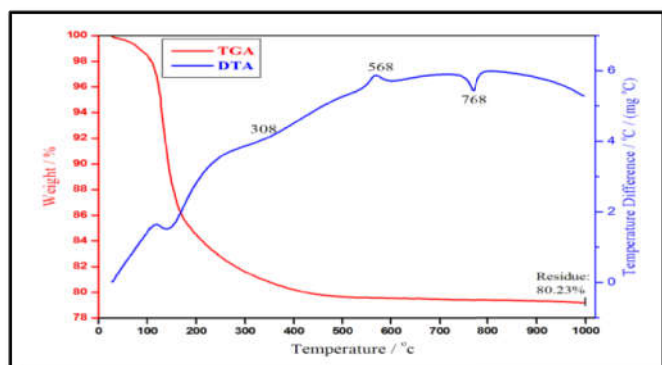


Figure 2 TGA and DTA scans for NB glass at 20 °C / min heating rate.

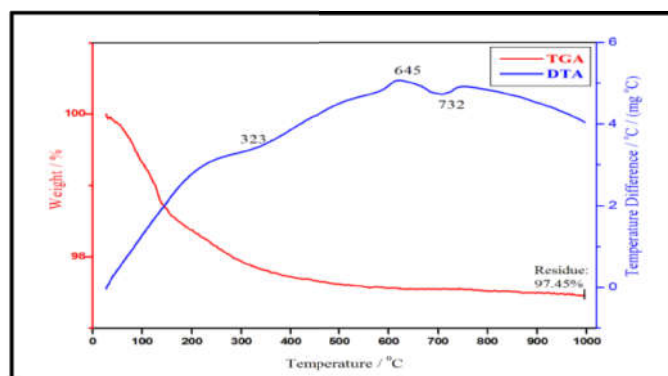


Figure 3 TGA and DTA scans for NBL3 glass at 20 °C / min heating rate.

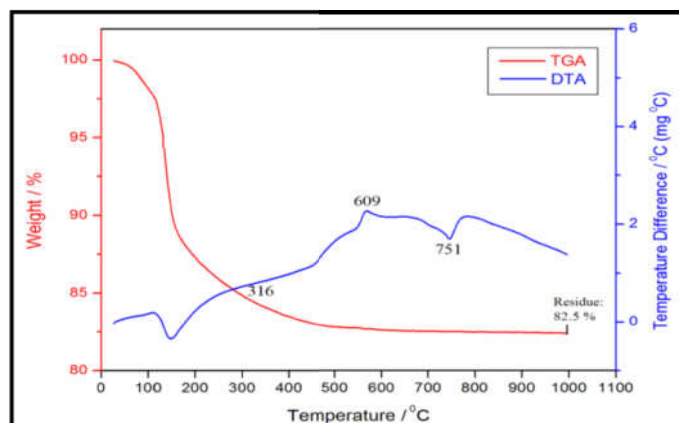


Figure 4 TGA and DTA scans for NBW3 glass at 20 °C / min heating rate.

**Table 1** The Values of glass transition temperature ( $T_g$ ), crystallization peak temperature ( $T_p$ ), melting temperature ( $T_m$ ) and thermal stability ( $\Delta T$ ) of various glass samples.

| Glass Samples label | Glass transition temperature $T_g$ / °C | Crystallization peak temperature $T_p$ / °C | Melting temperature $T_m$ / °C | Thermal stability $\Delta T$ / °C |
|---------------------|---|---|--------------------------------|-----------------------------------|
| NB                  | 308                                     | 568   | 768                            | 260                               |
| NBL 3               | 323                                     | 645   | 732                            | 322                               |
| NBW 3               | 316                                     | 609   | 751                            | 293                               |

The width of the glass transition region,  $\Delta T$ , is a measure of stability of glasses (Zhu *et al.*, 2003). Similarly, the observed increase in  $T_g$ , for glasses that are studied which is due to the destruction of non-bridging oxygen atoms (NBO) (Shapaan *et al.*, 2010). From this it is concluded that the strength of the glasses are increase with the doping of  $Li_2O$  and  $WO_3$  contents in sodium borate glass systems. From the above table it is also found that the thermal stability of glasses tends to increase with doping of  $Li_2O$  or  $WO_3$  content. This increasing trend of  $\Delta T$  suggests that the chemical bond strength of Li-O and W-O bonds in the glasses is stronger than that of B-O bonds (Alexsandrov *et al.*, 2011). The higher values of  $\Delta T$  correspond to delay in nucleation and thus, provide wider processing window for a glass composition to attain maximum densification. In the present study, increasing tungsten content in glasses decreases the value of  $\Delta T$ , thus implying towards degradation in sintering behavior of glasses (Ishu Kansal *et al.*, 2012). The thermal stability criterion  $\Delta T$  of glasses is larger than 100 °C, indicating that these glasses have good thermal stability and can easily be obtained in bulk forms (Gao Tang *et al.*, 2011). The larger  $\Delta T$  obtained for NBL glass has more thermal stability than NBW glass.



**Microhardness Studies**

The experimental values of microhardness ( $H_v$ ) and Meyer's index number (n) with various applied load for the NB, NBL and NBW glass series at room temperature are shown in table-2. The variations of microhardness with applied load for the undoped and doped of lithium oxide ( $Li_2O$ ) and tungsten trioxide ( $WO_3$ ) in sodium borate glass are drawn in Figs. 5 and 6.

Microhardness expresses the stress required to eliminate the free volume of the glass. The free volume in the glass is the openness of the glasses over that of the corresponding glasses (Varshneya *et al*, 1994). For all the glass systems, there is an increase in microhardness value (Figs 7&8) while increasing the applied load from 0.1 to 0.5Kg as well as with increasing the mol% of  $Li_2O$  and  $WO_3$  contents. Beyond 0.5Kg the value gets decreases, but when the load exceeds 1.0Kg, significant crack initiation and glass chipping occur and hardness tests could not be carried out.

The increasing value of microhardness makes the glass harder and vice versa. In all the studied glass systems the increase of the microhardness with increasing load is in agreement with the reverse indentation size effect (reverse ISE) (Hemalatha *et al*, 2009). The magnitude of  $H_v$  value is in order:  $NBL > NB > NBW$ . From the magnitude of  $H_v$ , with the effect of doping it can be concluded that NBL glasses possess higher rigidity than the NBW glasses. It is well known that the magnitude of microhardness related to bond energies (Yamane *et al*, 1974). According to Onitsch (Onitsch *et al*, 1944), work hardening exponent 'n' is less than 2 when the hardness increases with the increasing load. Since the values of n (Table 2) for NBL glasses are less than 2, the hardness of the material is found to increase with increase of load conforming the prediction of Onitsch.

**Table 2** Values of microhardness ( $H_v$ ) and Meyer's index number / work hardening exponent (n) for various glass compositions with different applied load at room temperature

| Glass Samples label | Microhardness $H_v$ /Mpa   |      |      |      |      | Meyer's index number/ Workhardening exponent (n) |
|---------------------|--|------|------|------|------|--|
|                     | 0.1  | 0.2  | 0.3  | 0.5  | 1.0  |  |
| NB                  | Load / (kg)  |      |      |      |      | 0.78   |
|                     | Na <sub>2</sub> O-B <sub>2</sub> O <sub>3</sub> (NB)                     |      |      |      |      |  |
|                     | 63.8   | 100  | 134  | 145  | 80.6 |  |
|                     | Na <sub>2</sub> O-B <sub>2</sub> O <sub>3</sub> -Li <sub>2</sub> O (NBL) |      |      |      |      |  |
|                     | 26.8   | 71.1 | 397  | 514  | 373  |  |
| NBL 2               | 29.3   | 102  | 468  | 558  | 445  | 1.49   |
| NBL 3               | 32.1   | 276  | 505  | 563  | 498  | 1.23   |
| NBL 4               | 55.3   | 365  | 586  | 608  | 509  | 0.38   |
| NBL 5               | 55.4   | 531  | 718  | 625  | 576  | 0.08   |
| NBW                 | Na <sub>2</sub> O-B <sub>2</sub> O <sub>3</sub> -WO <sub>3</sub> (NBW)   |      |      |      |      |  |
|                     | 31.6   | 34.4 | 35.9 | 75.6 | 56.6 |  |
|                     | 36.6   | 35.4 | 36.4 | 83.7 | 62.5 |  |
|                     | 40.4   | 43.6 | 59.5 | 150  | 72.8 |  |
|                     | 40.6   | 47.9 | 82.8 | 175  | 93.6 |  |
| NBW 5               | 50.9   | 86.7 | 115  | 263  | 142  | 2.34   |

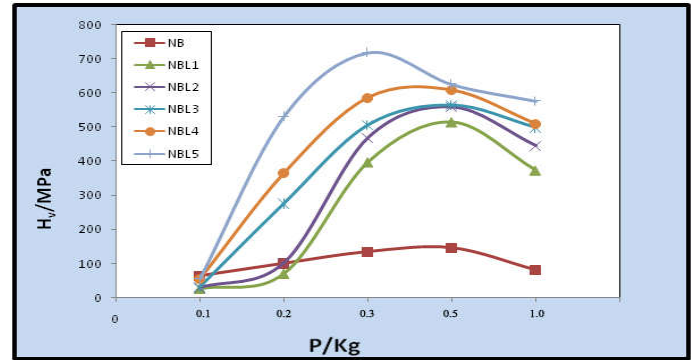


**Figure 5** Variation of microhardness ( $H_v$ ) versus load (P) for NB and NBL glasses at room temperature.

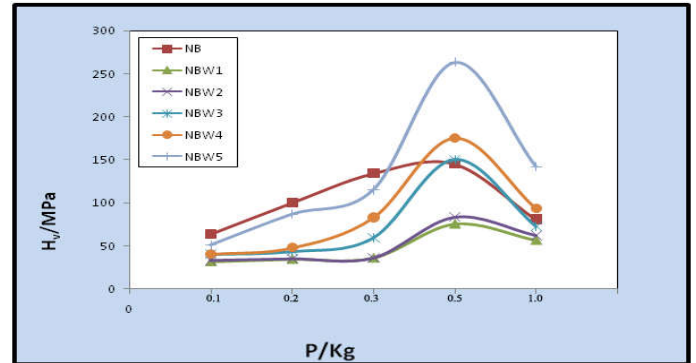


**Figure 6** Variation of microhardness ( $H_v$ ) versus load (P) for NB and NBW glasses at room temperature.

**FTIR Studies**

The FTIR transmittance spectra of NB, NBL3, and NBW3 glasses were recorded over the range of 400-4000  $cm^{-1}$  and are shown in Fig.7. The obtained transmission band and their assignments are summarized in tables 3.

In the studied glasses of NB, NBL and NBW, FTIR bands assignments have been revealed as follows:

The weak bands around 434-472  $cm^{-1}$  are assigned to the vibrations of Li cations through glass network which are attributed to Li-O-Li bonds (Edukondalu *et al*, 2013). The band 532-555  $cm^{-1}$  may be due to vibrations of sodium cations through the glass network. The band 692-702  $cm^{-1}$  can be attributed to B-O-B bond bending vibrations of bridging oxygen atoms (Vandana Sharma *et al*, 2012). The present FTIR spectra showed non-existence of band at 806  $cm^{-1}$ , which reveals the absence of boroxol rings in glasses and hence it consists of only  $BO_3$  and  $BO_4$  groups (Alemi *et al*, 2009). The peaks at 926-929  $cm^{-1}$  are assigned to the stretching vibrations of W-O and W=O bonds associated with  $WO_4$  and  $WO_6$  units, respectively (Celikbilek *et al*, 2013). The bands at 1159-1163  $cm^{-1}$  attributed to the vibrations of  $BO_4$  tetrahedra units. The band in the region 1329-1423  $cm^{-1}$  are attributed to the stretching vibrations of the B-O of trigonal ( $BO_3$ )<sup>3-</sup> units in metaborates, pyroborates and orthoborates groups (Gaafar *et al*, 2013). The bands from 1624-3847  $cm^{-1}$  are attributed to O-H bending that give rise to absorption in this region and the possibility of some adsorbed water (Vandana Sharma *et al*, 2012). In sodium borate glasses there are three types of structural groupings; namely boroxol rings, tetraborate units and diborate units. All of these groups share two distinct types of boron configurations;  $BO_3$  triangles and  $BO_4$  tetrahedra with

bridging oxygen ions for each type. In high-sodium borate glasses (20 mol% of Na<sub>2</sub>O), tetraborate groups are partially rearranged, and one Na<sub>2</sub>O forms two diborate units at the expense of a tetraborate unit, As a result, one Na<sub>2</sub>O forms two BO<sub>4</sub> units, which makes the network structure three-dimensional (Padmaja *et al*, 2009 and Krogh-Moe *et al*, 1969). The positive deviation in glass transition temperature is explained due to the increase in cross link density; hence increase in T<sub>g</sub> when compared with the end members. The Li<sup>+</sup> and Na<sup>+</sup> ion organized the structural arrangement of the planar BO<sub>4</sub> units slightly and favors the destruction of non-bridging oxygen in glass system. The destruction of non-bridging oxygen units causes the polymerization of the oxide network.

The increase in T<sub>g</sub> when compared with end members is attributed to the destruction of non-bridging oxygen BO<sub>3</sub> units in present glass system. FTIR studies in tungsten sodium borate glasses it was observed W<sup>6+</sup> prefers six-coordination and exhibits a transmittance band at 929 cm<sup>-1</sup>. In the presents study, the peak at 929 cm<sup>-1</sup> is assigned to the stretching vibrations of B-O linkages BO<sub>4</sub> tetrahedra overlapping with the stretching vibrations of WO<sub>6</sub> units (Edukondalu *et al*, 2013). Infrared investigations on present glass systems reveal no significant changes in the overall structure of the glasses with composition. These glasses contained BO<sub>3</sub> and BO<sub>4</sub> units of various types as di, tetra, penta and ortho borates groups (Balachandar *et al*, 2013)

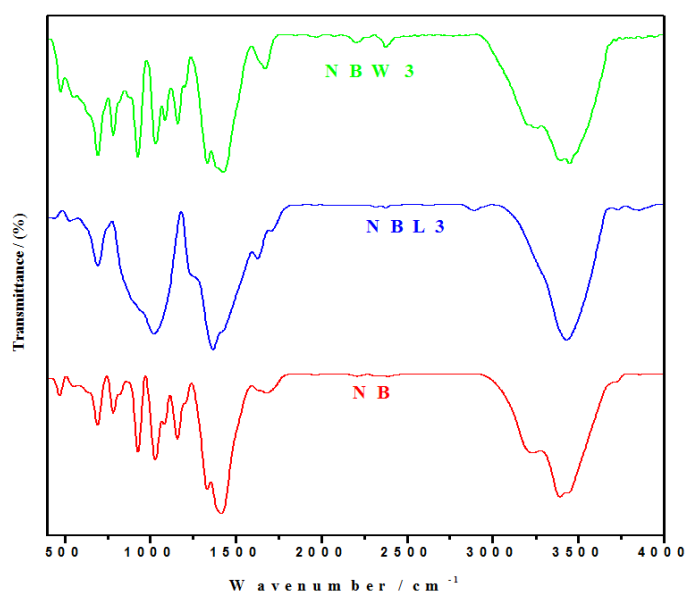


Figure 7 FTIR spectra of NB, NBL3 and NBW3 glasses.

Table 3 FTIR Bands assignment of Li<sup>+</sup> and W<sup>6+</sup> doped NB glass samples.

| Glass samples label | Band position / cm <sup>-1</sup>   | Band assignment   |
|---------------------|--|---|
| NB                  | 457-472  | Vibrations of Li cation.  |
|                     | 532-555  | Vibration of alkali Na cation.  |
|                     | 472, 555, 692, 785, 929, 1030, 1079, 1159, 1329, 1417, 1680, 3234, 3394.                         | Bending vibrations of B-O linkages in the borate network.   |
| NBL 3               | 926-929  | Stretching vibrations of W-O <sup>-</sup> and W=O bonds in tetrahedral [WO <sub>4</sub> ] units or octahedral [WO <sub>6</sub> ] units. |
|                     | 1030-1088  | Stretching vibrations of B-O bonds in BO <sub>4</sub> units from tri, tetra and penta borate groups.                                    |
|                     | 440, 532, 696, 1022, 136, 1627, 2378, 2894, 3434, 3731, 3847.                                    | Vibration of BO <sub>4</sub> tetra hedra.   |
| NBW 3               | ~1367  | Vibration due to triangular (BO <sub>3</sub> ) <sup>3-</sup> groups.  |
|                     | 1329-1423  | Stretching vibrations of the B-O of trigonal (BO <sub>3</sub> ) <sup>3-</sup> units in metaborates, pyroborates and orthoborates.       |
|                     | 478, 555, 694, 785, 928, 1034, 1088, 1161, 1334, 1427, 672, 2202,, 2378, 3265, 3452, 3876, 3945. | Stretching vibration of OH, molecular water,  |

## CONCLUSION

The effect of Li<sup>+</sup> and W<sup>6+</sup> ions doped with sodium borate glass has been investigated using TGA, DTA microhardness and FTIR measurements. The glassy state of the samples is characterized using TGA and DTA measurements. Further, the increasing behavior of T<sub>g</sub> and ΔT indicates the increasing strength and thermal stability of the investigated glass systems with the doping of Li<sub>2</sub>O and WO<sub>3</sub> content in sodium borate glass. From the ΔT values, it has been found that NBL glass has more thermal stability than NBW glass.

The microhardness measurements suggest that, beyond the load of 1.0 Kg, significant cracking occurred, which may be due to the release of internal stresses generated locally by indentation. Each glass exhibits a significant reverse ISE with indentation load. The increasing value of microhardness makes the glass harder.

The FTIR result suggests that the glass consists of BO<sub>3</sub>, BO<sub>4</sub>, Li-O-Li and W-O bridging bonds forming a large glass network. The characteristic boroxol ring (806 cm<sup>-1</sup>) was not observed in the present glass samples. Further, it has also been observed that Li<sub>2</sub>O and WO<sub>3</sub> contents help in converting BO<sub>3</sub> group to BO<sub>4</sub> units. This reveals that these ions also enter the glass structure as a network modifier. In the investigated glass system, the four-fold boron atoms dominated when compared with the three-fold ones. As most of the band positions remained the same in the infrared spectra, it can be concluded that the structure of the glasses is stable and the impact of variation of composition on the structure is not much significant.

## References

- Saddeek Y.B., Abousehly A.M., Hussein S.I. 2007. Synthesis and several features of the Na<sub>2</sub>O-B<sub>2</sub>O<sub>3</sub>-Bi<sub>2</sub>O<sub>3</sub>-MoO<sub>3</sub> glasses, *Journal of Physics D: Applied Physics*, 40, 4674.
- Balachandar L., Rramadevudu G., Shareefuddin Md., Sayanna R., Vendhar Y.C. 2013. IR analysis of borate glasses containing three alkali oxides, *Science Asian*, 39, 278-283.
- Saravanan S., Rajesh S., and Palani R. 2015. Thermal and Structural Properties of Mixed Alkali and Transition Metal Ions in Sodium Borate Glass, *International Journal Research and Review*, 3, 1-9.
- Abdel-Baki M., Salem A.M, Abdel-Wahab F.A., EIDIasty F. 2008. Bond character, optical properties and ionic conductivity of Li<sub>2</sub>O/B<sub>2</sub>O<sub>3</sub>/SiO<sub>2</sub>/Al<sub>2</sub>O<sub>3</sub> glass: effect of structural substitution of Li<sub>2</sub>O for LiCl, *Journal of Non-Crystalline Solids*, 354, 4527-4533.
- Varshneya A. 1994. Fundamental of inorganic glasses, Academic press, New York, 59.
- Bruker 2004. APEX2, SAINT and XPREP. Bruker AXS Inc., Madison, Wisconsin, USA.
- Marder S.R., Sohn J. E, Stucky G.D., 1991. Materials for Non- Linear Optics; American Chemical Society Washington, DC.
- Chenthamarai S., Jayaraman D., Subramanian C., and Ramasamy P. 2001. Mechanical and optical studies on pure and nitro doped 4-hydroxyacetophenone, material letters, 47, 247-251.
- Upender G., Chandra Mouli V. 2011 Optical, thermal and electrical properties of ternary TeO<sub>2</sub>-WO<sub>3</sub>-PbO glasses, *Indian Journal of molecular Structure*, 1006, 159-165.
- Sathyararyana T., Valente M.A., Nagarjuna G., Veeraiah N. 2013. Spectroscopic features of manganese doped tellurite borate glass ceramics, *Journal of Physics & Chemistry Solids*, 74, 229-235.
- Upender G., Vardhani C.P., Suresh S., Awasthi A.M., Chandra mouli V. 2010. Structure, physical and thermal properties of WO<sub>3</sub>-GeO<sub>2</sub>-TeO<sub>2</sub> glasses, *Material Chemistry & Physics*, 121, 335-341.
- Gaafar M.S., Saddeek Y.B., Abd El-Latif L. 2009. Ultrasonic studies on alkali borate tungstate glasses. *Journal of Physics & Chemistry and Solids*, 70, 173-179.
- Lide D. R. 2001. CRC Hand book of Chemistry and Physics, CRC press, (Ed.). Boca Raton.
- Upender G., Chinna babu J., Chandra mouli V. 2012, Structure, glass transition temperature and spectroscopic properties of 10Li<sub>2</sub>O-xP<sub>2</sub>O<sub>5</sub>-(89-x) TeO<sub>2</sub>-1CuO (5 ≤ x ≤ 25 mol%) glass system, *Spectra Acta Part A: Molecular & Bimolecular Spectra*, 89, 39-45.
- Hirashima H., Kurokawa H., Mizobuchi K., and Yoshida T. 1988. Electrical conductivity of vanadium phosphate glasses containing ZnO or GeO<sub>2</sub>, *Glastechnische Berichte*, 61(6), 151-156.
- Zhu D., Ray C. S., Zhou W., Day D. E. 2003. Glass transition and fragility of Na<sub>2</sub>O-TeO<sub>2</sub> glasses, *Journal of Non-Crystalline Solids*, 319, 247-253.
- Shapaan M., Ebrahim F. M. 2010. Structural and electric-dielectric properties of B<sub>2</sub>O<sub>3</sub>-Bi<sub>2</sub>O<sub>3</sub>-Fe<sub>2</sub>O<sub>3</sub> oxide Glasses, *Physica B*, 405, 3217-3222.
- Alexsandrov L., Komatsu T., Iordanova R., Dimitriav Y. 2011. Study of molybdenum coordination state and crystallization behavior in MoO<sub>3</sub>-La<sub>2</sub>O<sub>3</sub>-B<sub>2</sub>O<sub>3</sub> glasses by Raman spectroscopy, *Journal of Physics & Chemistry Solids*, 72, 263-268.
- Ishu Kansal, Ashutosh Goel, Dilshat U., Tulyaganov, Raghu Raman Rajagopal, Jose Ferreira M. F. 2012. Structural and thermal characterization of CaO-MgO-SiO<sub>2</sub>-P<sub>2</sub>O<sub>5</sub>-CaF<sub>2</sub> glasses, *Journal of European Ceramic Society*, 32, 2739-2746.
- Gao Tang, Huihua Xiong, Weichen, Lan. 2011. The study of Sm<sup>3+</sup>-doped low-phonon-energy chalcogenide glasses, *Journal of Non-Crystalline Solids*, 357, 2463-2467.
- Hemalatha P., Veeravazhuthi V., and Mangalaraj D., Benzyl S. 2009. Vickers microhardness study of nonlinear optical single crystals of doped and undoped isothiuronium chloride, *Journal of material engineering perform*, 18, 106-108.
- Yamane M., and Mackenzie J.D.1974.Vickers hardness of glass, *journal of non-crystalline solids*, 15, 153-164.
- Onitsch E.M. 1944. Strain rate Dependence of the hardness of glass and Meyers law, *Microscopie*, 2, 131-151.
- Edukondalu, Kavitha B., Samee M.A., Shaik Kareem Ahmed, Syed Rahman, Siva Kumar K. 2013. Mixed alkali tungsten borate glasses - Optical and structural properties, *Journal of Alloys & Compound*, 552, 157-165.
- Vandana Sharma, Supreet Pal Singh, Gurmel Singh Mudahar, Kulwant Singh Thind. 2012. Synthesis and optical characterization of silver doped sodium borate glasses, *National Journal of glass & ceramic*, 2, 133-137.
- Alemi A.A., Kafi-Ahmadi L., and karamipour Sh. 2009. Preparation and characterization of terbium oxide doped sodium tetra borate glasses, *International journal of crystal minimum*, 16, 1387-1393.
- Celikbilek M., Ersundu A.E., Aydin S. 2013. Preparation and characterization of TeO<sub>2</sub>-WO<sub>3</sub>-Li<sub>2</sub>O glasses, *Journal of Non-Crystalline Solids*, 378, 247-253.
- Gaafar M.S., Marzouk S.Y., Zayed H.A, Soliman L.I., Serag El-Deen A.H. 2013. Structural studies and mechanical properties of some borate glasses doped with different alkali and cobalt oxides, *Current Applied Physics*, 13, 152-158.
- Padmaja G., Kishtaiah P. 2009. Infrared and Raman Spectroscopic Studies on Alkali Borate Glasses: Evidence of Mixed Alkali Effect, *Journal of Physics and Chemistry A*, 113, 2397-2404.
- Krogh-Moe J. 1969. The structure of vitreous and liquids boron oxide, *Thermodynamic Acta*, 269-270, 457-46.

\*\*\*\*\*